scientific reports

Check for updates

OPEN

Investigating the effects of spring-loaded knee brace stiffness on gait biomechanics through predictive simulation

Kuan Wang[2,1]✉, Linlin Zhang[2], Leichao Liang[2], Xiaoyue Hu[2], Xinpeng Chen[3] & Huihao Wang[4]✉

This study aims to elucidate the biomechanical effects of varying spring-loaded knee brace (SLKB) stiffness on knee joint mechanics. This study combined musculoskeletal modeling with a direct collocation optimal control framework to perform a predictive simulation of walking under varied SLKB stiffness (0–1.0 Nm/deg), walking speeds (1.1–1.5 m/s), and slopes (level, 5°/10° uphill and downhill). A multi-term cost function minimized metabolic energy, muscle activation rates, actuator excitations, joint accelerations, and joint-limit penalties, yielding physiologically realistic trajectories that satisfied dynamic, path, and boundary constraints. Low-stiffness SLKBs closely matched the no-brace baseline, whereas increasing stiffness progressively restricted knee range of motion, induced minimal ground reaction force changes except under incline conditions, elevated knee flexor activations (biceps femoris, lateral gastrocnemius) for foot clearance, and reduced vastus medialis activity during inclined and declined walking. Crucially, medium to high-stiffness SLKBs produced consistent early-stance unloading of the knee vertical joint reaction force—up to 29.3% reduction uphill and 23.6% reduction downhill—although unloading effects attenuated or reversed in mid- and late-stance. Increasing SLKB stiffness influenced knee kinematics and muscle activations, with phase- and condition-dependent unloading effects, particularly during uphill walking. These findings suggest potential benefits for knee osteoarthritis, warranting in vivo validation and the development of subject-specific, condition-adaptive designs.

Keywords Direct collocation, Ground reaction force, Kinematics, Knee brace, Simulation

The knee joint is essential for human mobility. Anatomically, the knee joint comprises the femur, tibia and patella, together with ligaments that stabilize the joint and surrounding muscles such as the quadriceps, hamstrings and gastrocnemius, all of which contribute to the distribution and magnitude of loads experienced by the joint. These complex structure enables load-bearing and accommodates a wide range of motions required for daily activities, including ambulation across varied terrains and negotiation of inclines and declines. Degenerative conditions, particularly osteoarthritis, account for the majority of knee complaints. A recent systematic analysis projected that by 2050 knee osteoarthritis will affect over 642 million individuals worldwide, thereby imposing substantial socioeconomic burdens[1]. To support the joint, alleviate pain, and enhance stability, clinicians commonly prescribe knee braces[2,3]. Among these devices, spring-loaded knee braces (SLKBs) have emerged as innovative orthopedic aids that provide dynamic mechanical assistance. Each SLKB integrates a spring-loaded hinge that stores energy during knee flexion and releases it during extension, thereby delivering an extension-assistive moment that reduces joint loading across tibiofemoral compartments. This mechanism not only alleviates symptoms in conditions such as osteoarthritis, meniscal tears, and ligament injuries but also augments muscular support during activities like stair climbing, squatting, and walking. Crucially, the efficacy of SLKBs depends on

[1]Pudong Gongli Hospital, Shanghai University of Medicine & Health Sciences, Shanghai, China. [2]College of Rehabilitation Sciences, Shanghai University of Medicine and Health Sciences, Shanghai 201318, China. [3]School of Biomedical Sciences, The University of Queensland, St. Lucia 4072, Australia. [4]Shi's Center of Orthopedics and Traumatology (Institute of Traumatology, Shuguang Hospital), Shuguang Hospital Affiliated to Shanghai University of Traditional Chinese Medicine, Shanghai 201203, China. ✉email: Kuan__Wang@outlook.com; wangk_24@sumhs.edu.cn; huihaowang@126.com

their mechanical characteristics—particularly hinge stiffness—and the interaction of these properties with the knee's natural kinematics.

However, the interaction between SLKB stiffness and walking speed—and their combined impact on intra-articular forces and kinematic patterns—remains poorly understood. As walking speed increases, ground reaction forces (GRFs), muscle-generated loads, and inertial contributions undergo substantial changes[4], potentially altering the assistive or restrictive functions of SLKBs. Excessive hinge stiffness may impede physiological knee flexion and extension, leading to compensatory muscle activation or accelerated joint wear, whereas insufficient stiffness might fail to attenuate injurious loads during high-speed activities. Addressing this trade-off necessitates a simulation framework capable of realistically replicating the dynamic conditions encountered in daily locomotion.

Recent investigations have advanced our understanding of knee-brace biomechanics. Experimental trials have demonstrated that bracing can enhance joint stability and reduce pain, and biomechanical analyses have shown reductions in joint torque and contact forces during various movements[5,6]. While in vivo measurement of knee joint forces offers valuable insights for gait analysis, its reliance on invasive sensor implantation restricts widespread application[7,8]. Conversely, prior computational studies have primarily focused on isolated knee flexion–extension motions, with limited exploration of SLKB performance during functional tasks such as walking[9,10]. Moreover, few studies have concurrently examined the influence of brace stiffness and gait velocity within a unified simulation environment. This knowledge gap is critical, as an effective knee brace must perform reliably across diverse dynamic scenarios representative of daily life.

Computational simulation offers a noninvasive, highly controllable means to investigate joint mechanics under conditions that are difficult or impractical to reproduce experimentally. It enables systematic variation of parameters such as joint geometry and walking conditions, while capturing detailed muscle and contact force responses[11–13]. A central feature of our approach is predictive simulation enabled by the direct collocation method. Unlike traditional simulation techniques that relied on iterative approximations and simplifying assumptions, direct collocation provides a robust framework for managing the complex, multidimensional variables inherent in human motion[14]. Moreover, while clinical assessments focus largely on subjective pain metrics and gross functional scales, objective quantification of internal joint loading through noninvasive computational modeling remains relatively rare. Direct collocation methods present an opportunity to bridge this gap by enabling high-fidelity simulation of muscle and ligament contributions under diverse loading scenarios. This method discretizes the gait cycle into finite segments, enabling simultaneous optimization of state and control variables throughout the motion[15]. We implemented direct collocation within a detailed musculoskeletal model of normal walking, systematically varying walking speed and SLKB stiffness. This framework captures rapid, subtle variations in joint kinematics and muscle activations that occur during everyday activities.

Research on knee brace biomechanics has employed a variety of methodological approaches, yet many prior investigations have been limited in scope. Experimental gait analyses have often focused on the effects of limited commercial brace designs, reporting changes in joint kinematics or GRFs under level-walking conditions[16]. Computational studies, particularly those using finite element methods, have largely concentrated on quasi-static evaluations of brace–limb interaction, providing valuable insights into localized stress distributions but offering limited information on dynamic gait performance with active muscle involvement[17,18]. Stoltze et al[19]. examined an unloading knee brace in patients with knee osteoarthritis at self-selected walking speeds, without assessing controlled gait speeds or varied slope conditions. Other biomechanical assessments have investigated brace function during discrete, high-demand tasks such as jumping or squatting, but have not systematically controlled walking speed or explored a broader range of locomotor conditions[10,20,21]. Scenarios common to daily life—such as uphill and downhill walking while wearing a knee brace—have not been extensively studied, despite their clear relevance to brace performance and user mobility. The present study addresses these gaps by employing a validated full-body musculoskeletal model to systematically vary SLKB stiffness across multiple controlled walking speeds and slope conditions, enabling a comprehensive evaluation of kinematics, GRFs, and muscle activations in gait contexts that closely reflect real-world demands.

This study aims to elucidate the biomechanical effects of varying SLKB stiffness on knee joint mechanics. We integrated musculoskeletal modeling with direct collocation optimization to simulate normal gait across a spectrum of walking speeds and brace stiffness configurations. By isolating the individual contributions of speed and stiffness, our approach quantifies detailed outcomes—joint angles, internal forces, and muscle activations—to reveal how stiffness modulates tibiofemoral loading. These insights can guide the design of more effective spring-loaded knee braces and inform clinical decision-making.

Methods

In this study, we simulated the biomechanical effects of spring-loaded knee braces (SLKBs) with varying stiffness on level and inclined walking at different speeds. We integrated an open-source musculoskeletal model with a direct collocation optimal control framework for multibody dynamics simulation (Fig. 1). Our approach generated physiologically realistic gait trajectories that satisfied dynamic constraints while systematically accounting for variations in SLKB stiffness.

The optimal control problem was formulated by defining state variables—including joint positions and velocities for all degrees of freedom (DoFs), normalized tendon forces, and muscle (or torque-actuator) activations—and control variables such as the time derivatives of muscle activations, torque-actuator excitations, joint accelerations, and tendon force rates. The system dynamics are governed by

$$M(q)\ddot{q} + C(q,\dot{q}) + G(q) = \tau$$

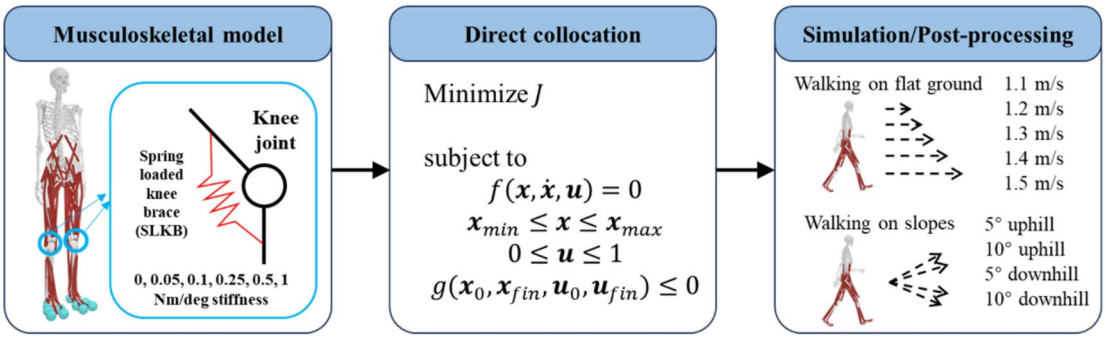

Figure. 1.. Simulation conditions and optimization scheme.

where $M(q)$ is the mass matrix, $C(q, \dot{q})$ incorporates Coriolis and centrifugal effects, $G(q)$ represents gravitational forces, and τ denotes the generated torques and external force such as GRFs. In addition to dynamic constraints, we enforced a series of path constraints to guarantee physiological fidelity at every point in the gait cycle within the direct collocation framework. Muscle activations and torque-actuator excitations were limited between zero and one, preventing nonphysical levels of neural drive or assistive torque. Joint kinematics—such as hip, knee, and ankle angles and angular velocities—were confined to anatomically defined ranges derived from cadaveric studies and in vivo measurements, thereby avoiding hyperextension or impingement[14]. Muscle-tendon forces were also bounded by their maximum isometric and dynamic capabilities, ensuring that fibers did not generate implausible loads. In addition to the path constraints described above, we enforced boundary conditions that captured the symmetry of a half-cycle walking simulation. Specifically, the generalized coordinates and velocities at the end of the simulated half-cycle were set to mirror those at the start, with left and right limb joint angles swapped and angular velocities sign-reversed to reflect contra-lateral symmetry. The horizontal pelvis translation advanced by half the prescribed stride length, ensuring that the average forward velocity over the half-cycle equaled the target walking speed. Finally, we adjusted the gravity vector orientation to represent level, uphill, or downhill slopes, guaranteeing that foot–ground interactions corresponded to the intended incline.

Our simulation framework was constructed upon an open-source musculoskeletal model (Primary model) that represents the entire lower extremity based on OpenSim 2392 model, along with a torque-actuated upper body constructed by Falisse et al.,[22,23]. The musculoskeletal model has been validated in terms of GRFs, joint dynamics, and muscle activation patterns under various walking speeds[14,23]. The musculoskeletal model comprises 20 rigid body segments, including the pelvis, trunk, bilateral femurs, tibias, taluses, calcanei, foot segments, as well as upper limb segments such as the humeri, forearms, and hands. It features a total of 31 degrees of freedom, incorporating a 6-DoF pelvic root, bilateral hip joints with 3 DoF each, knee joints with 1 DoF each, ankle joints with 1 DoF each, subtalar and metatarsophalangeal joints with 1 DoF each per side, a 3-DoF lumbosacral joint, and shoulder and elbow joints. In the model, each foot was represented by two segments, the forefoot and the toes. The forefoot contains four distributed contact sphere elements, while the toe segment includes two contact sphere elements according to Falisse et al.[23]. Ninety-two muscle–tendon units actuate the lower limbs, and several ideal torque motors assist the upper limb joints. To simulate foot–ground contact, six contact spheres are affixed to each foot with Hunt-Crossley model to represent contact force[14,24]. The skeletal segments are defined with physiological inertial properties, and the overall body mass is set at 62 kg. Muscle activation dynamics were modeled using established neural excitation and force-production models with polynomial approximations for muscle moment arms[14,25].

In this study, we varied three experimental factors—SLKB stiffness, walking speed, and slope angle—to assess their combined effects on gait biomechanics. Previous studies have reported knee-brace stiffness values in the range of approximately 0.05 to 0.3 Nm/deg[9,10,26,27], based on experimental measurements and manufacturer specifications. Guided by these findings, we selected SLKB stiffness levels of 0.05, 0.10 and 0.25 Nm/deg to represent the lower, mid, and upper bounds of the reported range. In addition, higher stiffness levels of 0.50 and 1.00 Nm/deg were included to enable parametric exploration of brace performance, thereby assessing potential effects under more extreme assistive conditions. The SLKB was set with bidirectional elasticity, enabling it to generate supportive moments during both knee flexion and extension. The typical walking speed is about 1.3 m/s[28]. Thus, we tested velocities of 1.1, 1.2, 1.3, 1.4, and 1.5 m/s to encompass the range encountered in daily activities. To examine incline effects, we conducted gait simulations on 5° and 10° uphill and downhill slopes. Trials without an SLKB (0 Nm/deg stiffness) served as the baseline condition, as this configuration has been validated to reproduce physiologically natural walking mechanics[14]. Additionally, to capture variability in body morphology across individuals, a set of ten skeletal models was derived from a SKEL-based framework[29]. Sampling was guided by the principal morphological dimensions, yielding a balanced representation of male and female body shapes. These models were subsequently aligned with the OpenSim musculoskeletal environment to generate individualized simulations. The sampled cohort had an average height of approximately 1.71 ± 0.08 m and a mean body mass of 71.4 ± 13.5 kg. The resulting models were then employed to examine gait dynamics under the two extreme brace stiffness levels (0 and 1.0 Nm/deg).

Central to our optimal control formulation is the cost function, which seeks to minimize a weighted combination of biomechanical criteria. In musculoskeletal simulations, the cost function is designed to capture essential biomechanical and physiological principles. In this study, the energy term estimates the metabolic power needed for muscle activation, force production, and posture maintenance under different loading conditions, which encourages movement patterns that mirror the energy-efficient strategies humans naturally employ. The regularization terms on control inputs and on the derivatives of state variables smooth out neural command signals and kinematic transitions to reflect the limited rate at which muscle excitation can change and the viscoelastic damping behavior of muscle–tendon complexes. The joint limit penalty assigns large costs to configurations that exceed anatomical ranges, ensuring that joint angles stay within safe, physiologically plausible limits. Together, these elements drive the optimizer to generate motion trajectories that reproduce walking kinematics and kinetics while respecting the energetic economy, neuromuscular control constraints, and anatomical boundaries inherent in real human movement[14]. Mathematically, the cost function is expressed as

$$J = \int_0^{t_f} \left(w_1 \dot{E}^2 + w_2 a^2 + w_3 e_a^2 + w_4 u_a^2 + w_5 T_p^2 \right) dt$$

where t_f is the gait cycle duration, $\dot{E}$ denotes the metabolic energy rate, a is the muscle activation rate, e_a represents the excitation for the torque actuators, u_a denotes joint acceleration, T_p corresponds to passive torques arising from joint limits, and w_{1-5} are empirically tuned weights (500, 2000, 1 000 000, 50 000, and 1000, respectively) to ensure that simulated energetic and kinematic characteristics align with experimental observations. An additional sensitivity analysis was performed by varying w_{1-5} by ± 50% in gait simulations with varying brace stiffness on 5° and 10° uphill slopes.

The entire computational workflow was implemented in Python. We leveraged the CasADi library to symbolically formulate the optimal control problem and to perform algorithmic differentiation and direct collocation on muscle-driven dynamics[30]. This optimization engine was then connected to OpenSimAD, a differentiable extension of the OpenSim simulation framework, which provides analytic gradients of musculoskeletal model outputs with respect to states and controls[31]. By using CasADi's efficient solver infrastructure with OpenSimAD's gradient, a fully differentiable pipeline was established for computing energy-optimal muscle excitations and joint kinematics. We discretized the half-gait cycle into 50 nodes using third-order polynomial interpolation to capture critical events such as heel strike and heel-off. An initial guess for state and control trajectories was generated from experimental walking datasets, providing a reliable starting point[14]. The resulting nonlinear programming (NLP) problem—comprising decision variables, dynamic and path constraints, and boundary conditions—was solved via the IPOPT interior-point algorithm until achieving an optimality-gap tolerance of 1×10^{-3}[32].

After simulation, we reconstructed the half-cycle outputs into a full gait cycle spanning one right foot contact to the next. We then extracted key biomechanical metrics: joint kinematics (hip, knee, and ankle flexion/extension angles), three-dimensional GRFs, temporal profiles of muscle activations, and joint reaction forces (JRFs) computed through OpenSim's joint reaction analysis[33].

Simulations were executed on a high-performance laptop equipped with an AMD Ryzen 9 7945HX processor and 64 GB of RAM. This integrated methodological framework enabled a rigorous assessment of SLKB biomechanical impacts across diverse conditions, yielding insights pertinent to clinical interventions and device engineering.

Results

In level walking simulations, models with lower SLKB stiffness produced joint kinematics similar to the baseline condition (Fig. 2). As SLKB stiffness increased, the knee's range of motion decreased markedly (Fig. 3). At 1.3 m/s, the average knee extension angle over one gait cycle was –22.2°, –21.2°, –20.2°, –17.8°, –18.8°, and –9.4° for SLKB stiffness values of 0, 0.05, 0.10, 0.25, 0.50, and 1.00 Nm/deg, respectively. Compared with level walking, both average hip and knee angles increased during 5° and 10° uphill as well as 10° downhill walking.

SLKBs with low stiffness exhibited minimal deviations from baseline GRFs in the normal direction (Fig. 2). During 1.3 m/s walking on a 5° uphill slope, the first peak of the normal GRF decreased for SLKB stiffnesses of 0.10, 0.25, 0.50, and 1.00 Nm/deg relative to baseline. On a 10° uphill slope at the same speed, only the 1.00 Nm/deg configuration produced a smaller first peak of the normal GRF compared with baseline. Due to the application of the knee brace, both kinematics and GRFs were altered, which in turn led to corresponding changes in the computed net joint moments, as illustrated in Fig. 4.

High-stiffness SLKBs induced larger changes in muscle activation and muscle force patterns compared with the no-brace baseline (Figs. 5 and 6). Most SLKB configurations increased the mean activation of knee flexors—including the short head of the biceps femoris, and the lateral gastrocnemius. In contrast, during 5° uphill, 10° uphill, and 10° downhill walking, SLKBs reduced activation of the knee extensor, e.g., vastus medialis.

The peak knee joint reaction force predicted by the primary model was comparable to that reported in the datasets[34] for a subject whose height, body mass, and walking speed were similar to those of the model used in this study (Fig. 7). Since SLKB substantially altered both kinematic and kinetic patterns, conventional gait-cycle segmentation was no longer applicable. Based on the GRF profiles observed in this study, we divided the vertical JRF into three stance-phase intervals (0–20%, 20–40%, and 40–60%) to approximate the early, mid-, and late-stance phases for convenience (Figs. 7 and 8). During the 0–20% phase of the gait cycle, 5° uphill walking produced average knee joint vertical JRF changes of + 0.2%, – 2.3%, – 18.3%, – 21.9%, and – 29.3% relative to baseline for SLKB stiffnesses of 0.05, 0.10, 0.25, 0.50, and 1.00 Nm/deg, respectively. In 10° uphill walking,

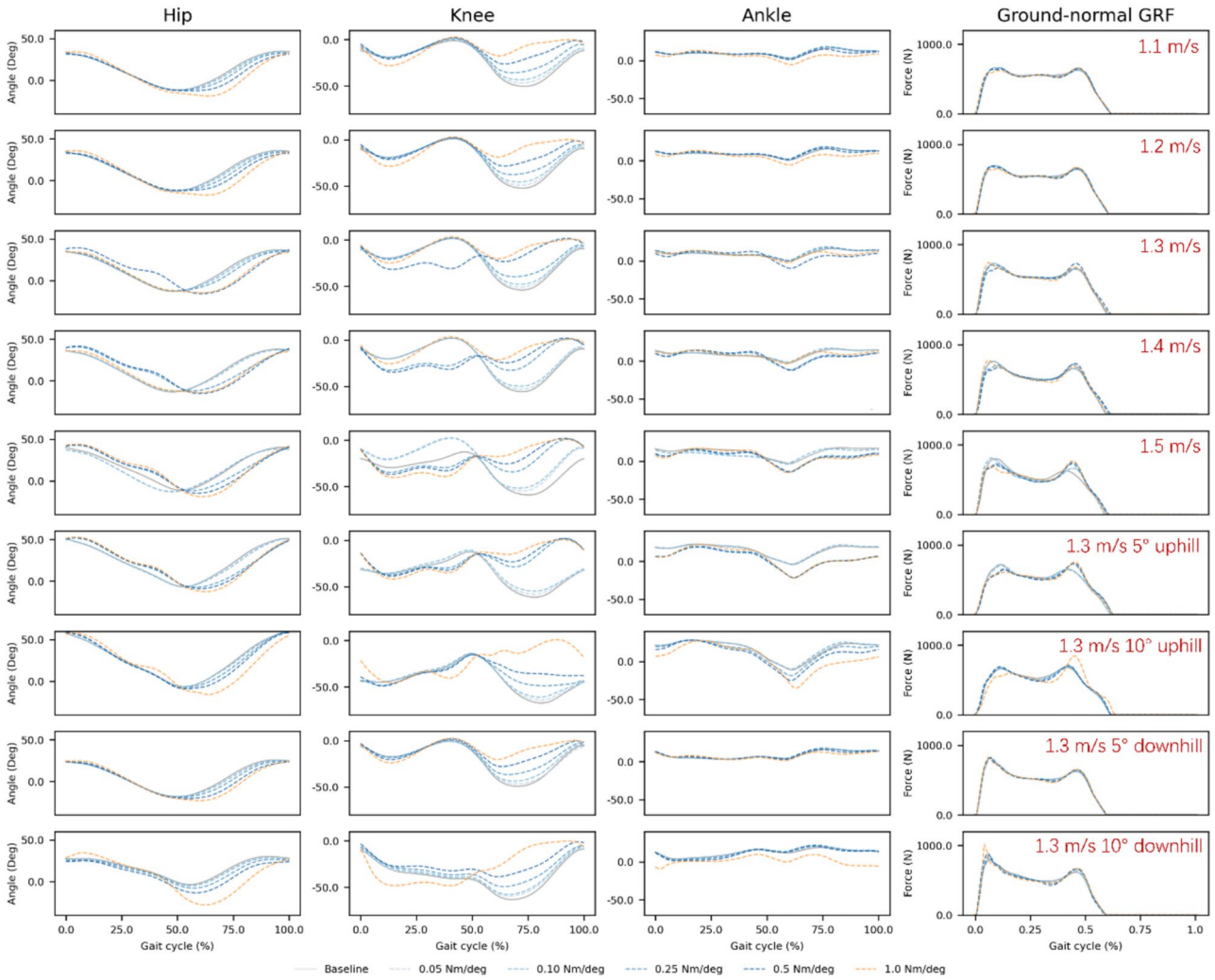

Figure. 2.. Kinematics and normal component of the ground reaction force (GRF) in various walking conditions with different knee brace stiffness predicted by primary model.

the corresponding changes were − 0.5%, − 1.1%, − 3.4%, − 7.2%, and − 22.9%. Sensitivity analysis revealed that varying the weights of cost function by ± 50% show consistent unloading effect of brace with 0.5 Nm/deg and 1.0 Nm/deg stiffness in uphill walking during the 0–20% phase of the gait cycle (See Supplementary Information). For 5° downhill walking, average knee joint vertical JRF changes were + 0.6%, − 2.2%, − 3.4%, − 5.8%, and − 10.4%, whereas 10° downhill walking yielded − 1.3%, − 6.2%, − 13.7%, − 19.2%, and − 23.6%. During the 20–40% phase, the unloading effect of knee joint was attenuated and was absent at 1.00 Nm/deg SLKB stiffness during downhill walking. During the 40–60% phase, SLKB generally increased vertical JRFs of knee joint compared with baseline (Fig. 8).

Discussion

This study leveraged musculoskeletal modeling integrated with direct collocation optimization to simulate normal walking under varied conditions and SLKB stiffness configurations. Previous knee-brace studies have predominantly investigated motions involving large knee-flexion angles[9,20]. By contrast, this work systematically evaluated SLKB effects on walking at various speeds and on uphill and downhill slopes. The results demonstrated how different brace designs influence knee mechanics during gait. These findings lay the groundwork for more tailored and effective interventions using SLKBs or similar knee-assistive devices.

One significant effect of SLKBs is their joint-limiting function. We found that SLKBs not only significantly reduced the knee's range of motion but also altered hip excursion, reflecting the cooperative action of these joints. During level-ground walking, the joint-limiting effect became more pronounced with increasing SLKB stiffness. However, knee flexion during the swing phase is essential for foot clearance[35]. To overcome SLKB resistance and achieve adequate flexion, we observed increased activation of knee flexor muscles—specifically the biceps femoris (short head) and lateral gastrocnemius—relative to the no-brace baseline in most level-ground scenarios. Therefore, SLKBs with high linear stiffness may not be ideal for effortless level-ground ambulation.

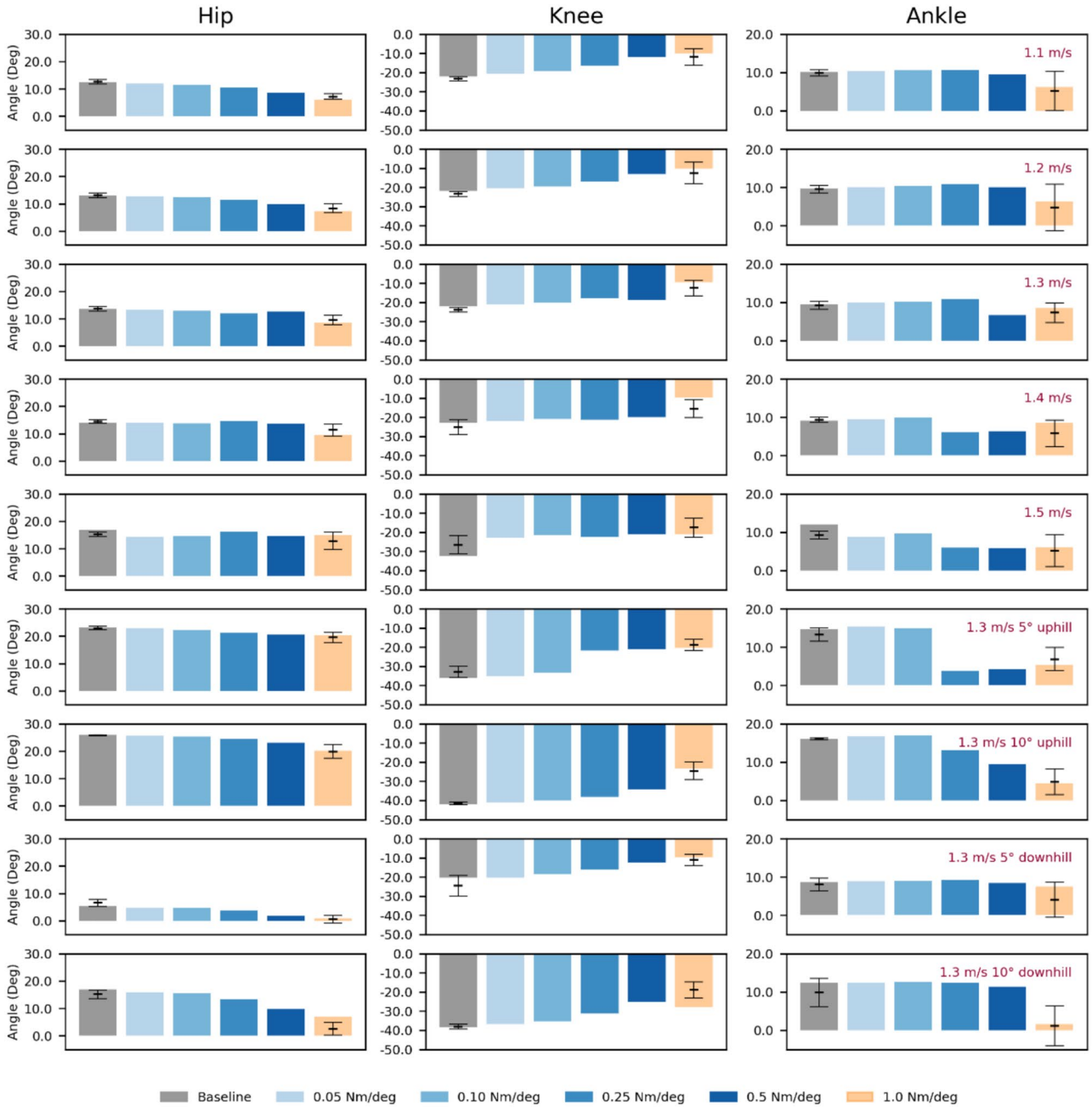

Figure. 3.. Averaged kinematics of various walking conditions with different knee brace stiffness. Bars show the predictions of the primary model. Horizontal markers and lines denote mean ± standard deviation predicted by additional models under two extreme brace stiffness levels (0 and 1.0 Nm/deg).

Conversely, when the goal is to restrict the knee near a neutral position—for example, in the management of bone fractures or ACL/PCL injuries—SLKBs could be beneficial.

This study found that SLKBs reduced the first peak of knee joint vertical JRF during level-ground walking. This outcome aligns with previous work reporting a 7.9% reduction in peak vasti muscle activation and up to a 26.3% decrease in the first peak of knee compressive force when using a knee brace[36]. Theoretically, knee JRF arises from the combination of foot–ground impact and muscle force loading across the joint. In the unbraced condition, knee extensor muscles act like a spring to attenuate impact during foot contact[37]. By defining the SLKB's neutral angle as an unloaded spring position, the device can partially assume the role of the extensor muscles, thereby lowering knee joint vertical JRF. Similar unloading effects have been observed in studies of SLKB-assisted push-off and sit-to-stand movements[9,20]. However, during walking, the brief duration and modest magnitude of knee flexion induced by foot contact limit SLKB efficacy. In our simulations of level-ground gait, low-stiffness SLKBs failed to consistently reduce the first vertical JRF peak of knee joint, and only the 1.0 Nm/deg configuration achieved reliable unloading during the early-stance phase. Moreover, during mid- and late-

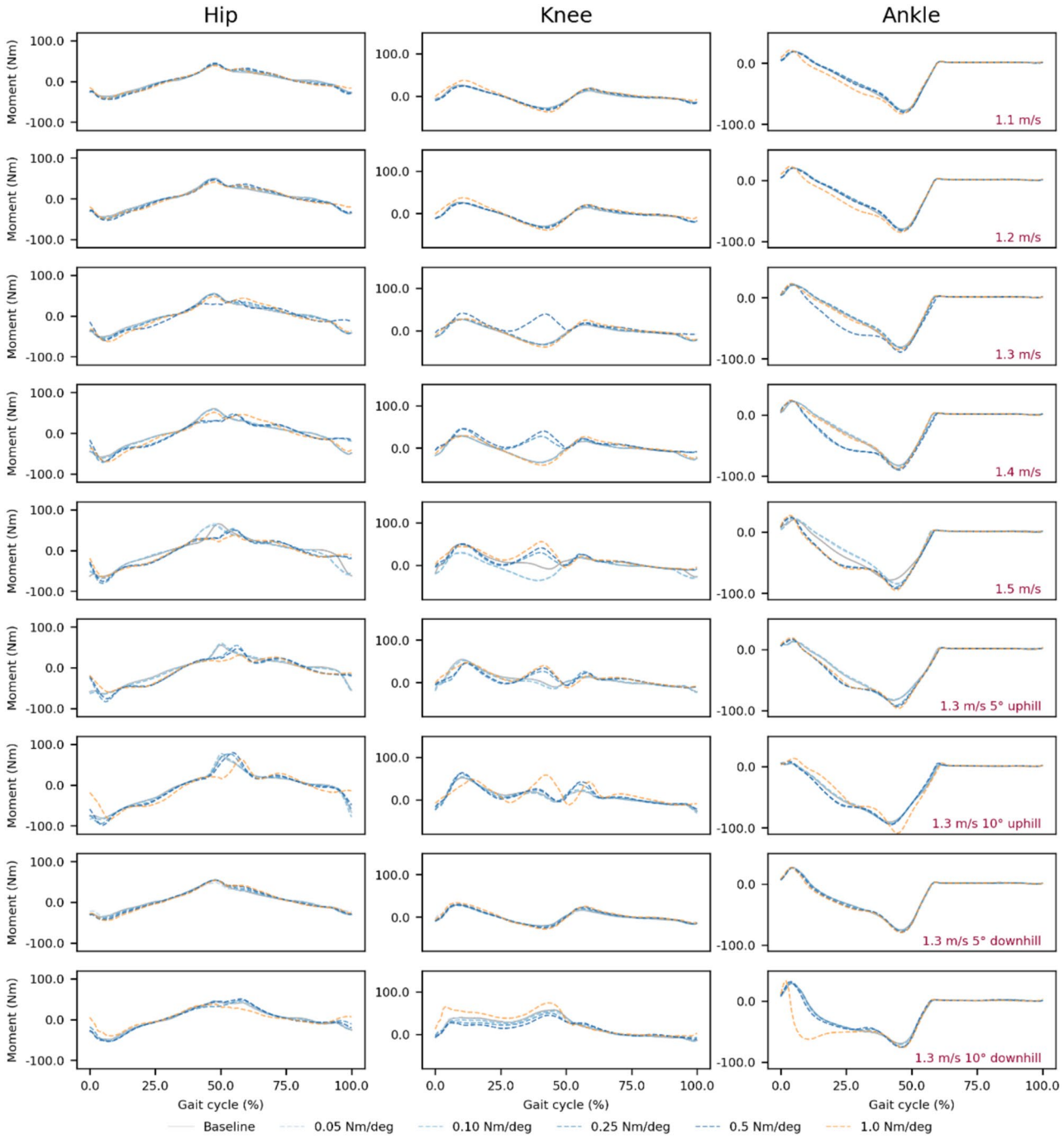

Figure. 4.. Joint moment in various walking conditions with different knee brace stiffness predicted by primary model.

stance phase—particularly at higher walking speeds—SLKBs tended to increase vertical JRF of knee joint. These findings indicate that SLKB-mediated reduction of the first JRF peak of knee joint is neither robust nor pronounced in level-ground walking. This theoretical insight helps explain why patients with knee osteoarthritis may not experience immediate pain relief from SLKB[36], and underscores the need for condition-adaptive knee-brace designs.

We also observed that medium and high-stiffness SLKBs reduced the first vertical JRF peak of knee joint during downhill walking. Although this unloading effect was smaller than that seen in uphill walking, it remained consistent across 5° and 10° declines. Downhill gait induces greater knee flexion angles than level walking[38], requiring stronger activation of knee extensors to return the joint to neutral. Under these conditions, the SLKB augments extensor torque and diminishes knee JRF. Similar to level walking, the unloading effect of knee joint dissipated or became inconsistent during the mid- and late-stance phases, indicating limited benefit of SLKBs in the later phases of downhill gait.

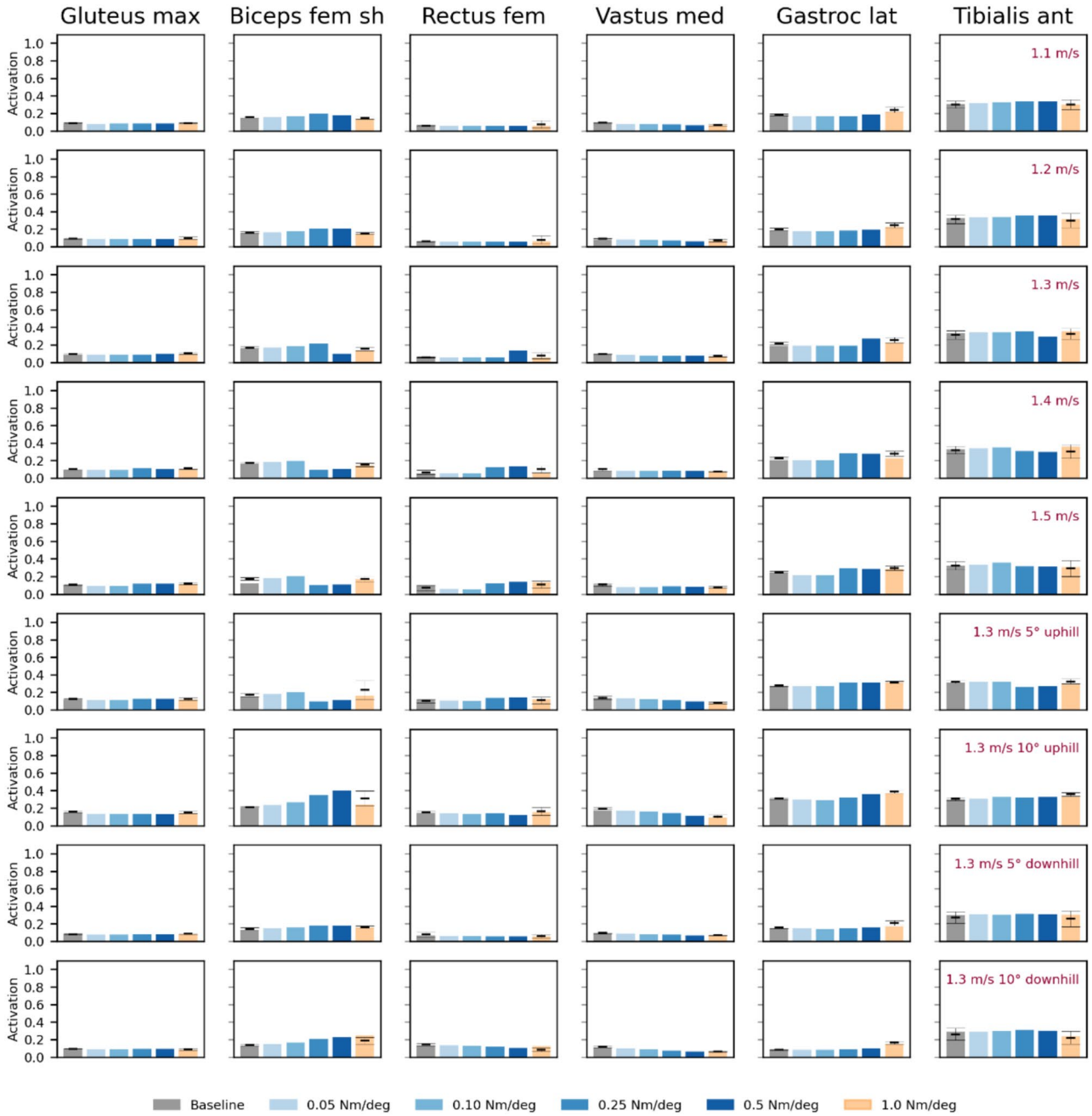

Figure. 5.. Averaged muscle activities of various walking conditions with different knee brace stiffness. Bars show the predictions of the primary model. Horizontal markers and lines denote mean ± standard deviation predicted by additional models under two extreme brace stiffness levels (0 and 1.0 Nm/deg).

The core finding of this study is that SLKBs reduced the first impact peak of knee joint vertical JRF during uphill walking. The knee naturally flexes more during uphill gait than in level-ground walking[39], requiring increased work by the knee extensor muscles. Our muscle activation data corroborated this result, in which vastus medialis activity in the no-brace condition was higher during the early-stance phase of uphill walking compared with level-ground gait. Under these conditions, SLKBs provided greater assistance in reducing the JRF generated by the extensor muscles. Moreover, this unloading effect remained consistent across both 5° and 10° uphill slopes and across the most SLKB stiffness levels tested. These results suggest that SLKBs could help unload the knee joint for patients with knee osteoarthritis during uphill ambulation. On the other hand, because knee osteoarthritis pain can be patello-femoral driven, changes in knee flexion angle may influence the patellar moment arm and quadriceps force. Accordingly, reductions in tibio-femoral joint reaction forces could be accompanied by shifts in patello-femoral loading, which should be taken into account when interpreting the overall unloading effects.

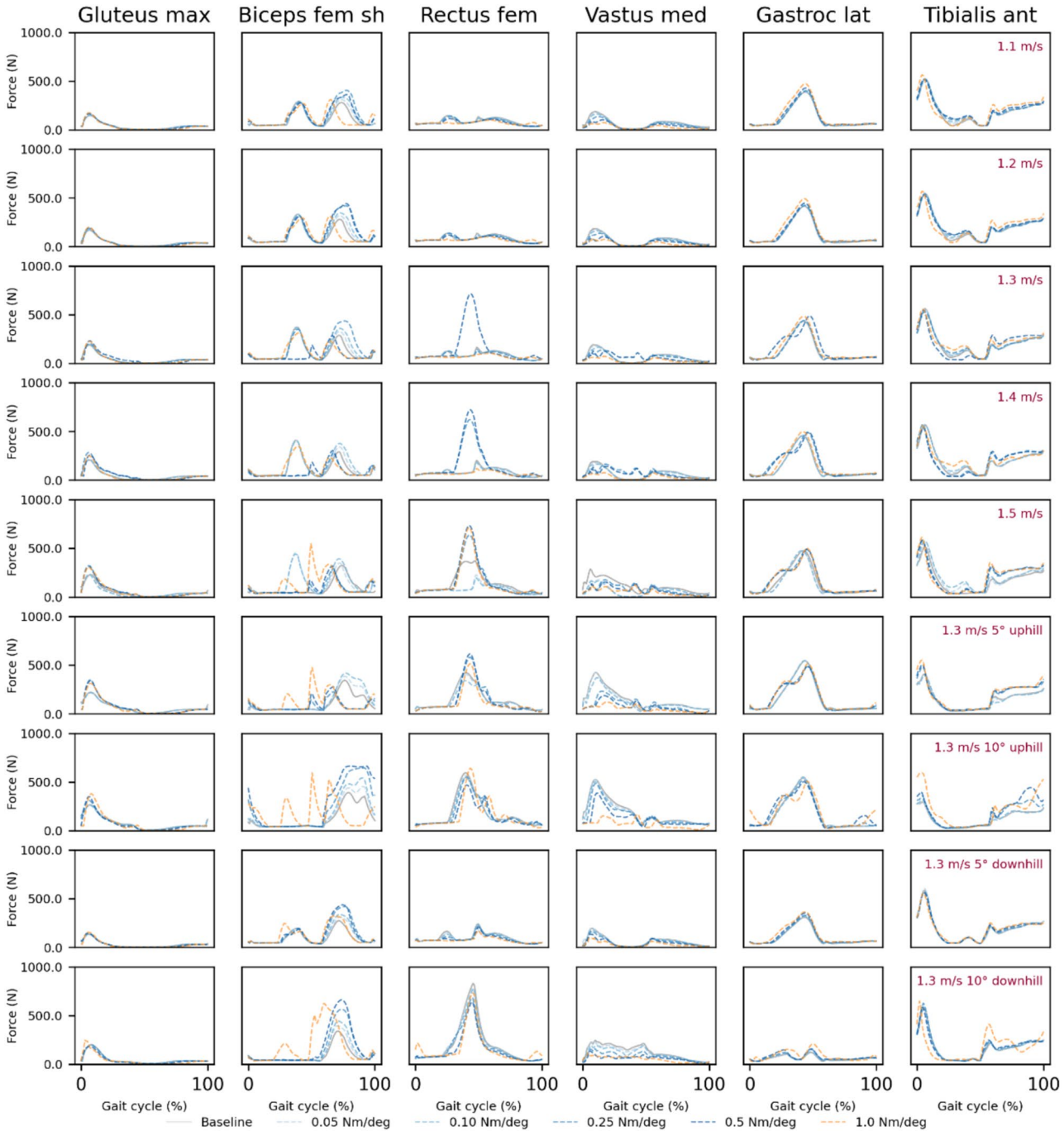

Figure. 6.. Muscle Force of various walking conditions with different knee brace stiffness predicted by primary model.

This study has several limitations. First, it relied on computational simulations with a relatively small virtual cohort. Future work will incorporate experimental data from a larger and more diverse population to corroborate the model predictions, assess inter-individual variability, and enhance the generalizability of the findings. Nevertheless, by systematically varying SLKB stiffness, walking speed, and slope parameters, we generated theoretical insights that can guide and streamline the design of subsequent in vivo studies. Second, we employed a combined cost function to simulate gait that—while representative of overall physiological demands—may not capture individual variations in motor control. Future in vivo research should incorporate subject-specific conditions to better tailor SLKB performance. Another limitation was that real SLKBs may exhibit hysteresis and preload, which our current model does not capture. Hysteresis would effectively increase damping and could reduce unloading. Quantifying this effect requires experimental brace characterization, which represents an important future direction. The findings of this study should be interpreted with appropriate caution. In this study, internal quantities such as knee joint reaction forces and muscle forces have not yet been directly

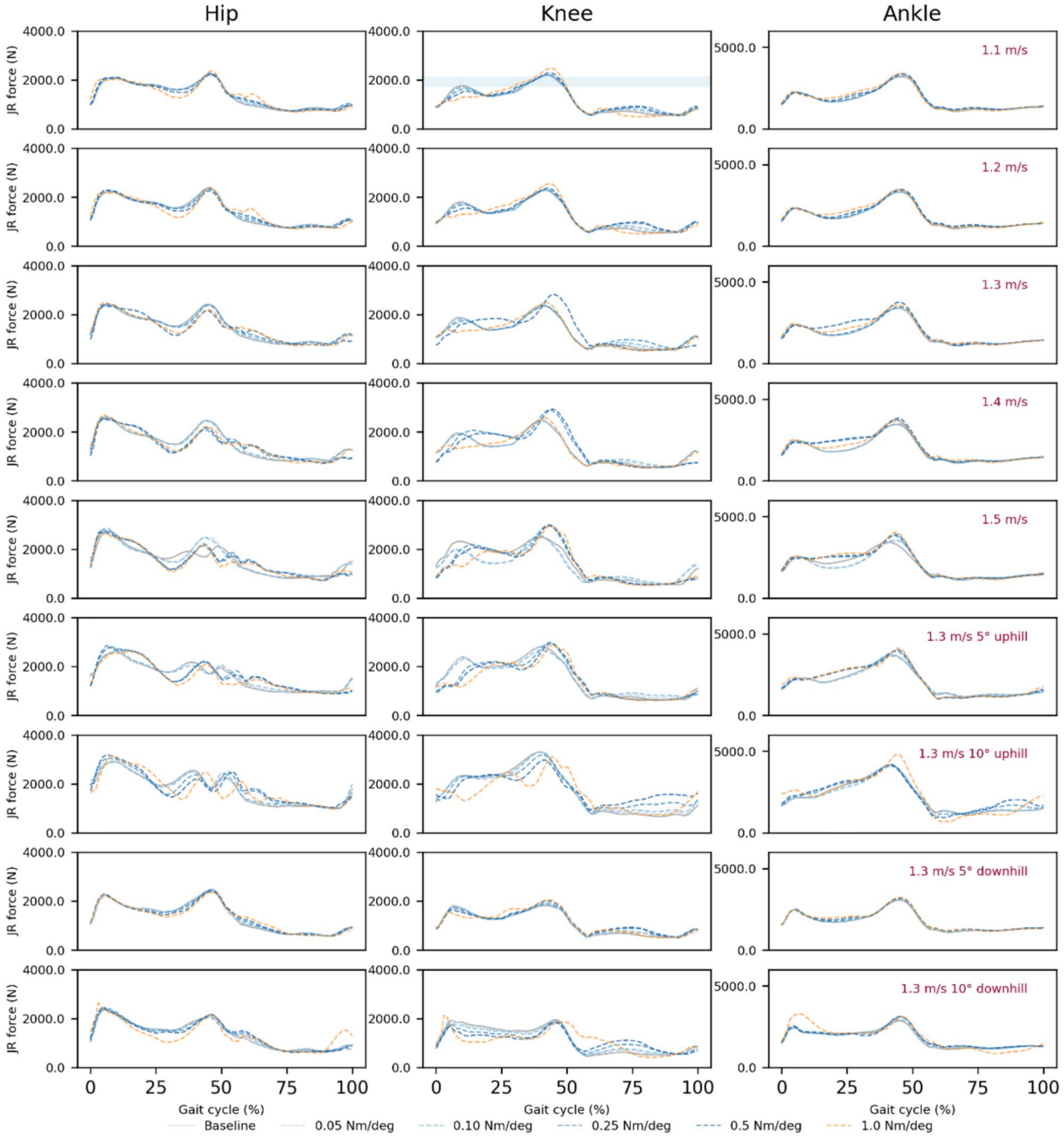

Figure. 7.. Vertical joint reaction (JR) force of various walking conditions with different knee brace stiffness predicted by primary model. The light blue horizontal band represents the range of peak in vivo knee joint reaction forces over a gait cycle, as reported in the datasets[34] for a subject with height, body mass, and walking speed comparable to those of the model used in this study.

compared with in-vivo benchmarks under brace-wearing conditions. However, to strengthen the study, we compared our baseline model predictions with in-vivo knee joint reaction force data reported in the literature for a similar walking condition. While not identical to the brace-wearing scenario, this comparison provides meaningful support for the validity of the baseline model. Future work will incorporate instrumented implant data or cadaveric experiments under brace-wearing conditions to further advance internal validation.

In terms of brace modelling, the spring moment is applied directly to the tibio-femoral joint without accounting for strap compliance or brace migration. This simplification may lead to an overestimation of the external extension moment, particularly during the swing phase when brace migration occurs. As a result, the predicted increase in biceps femoris activation may be influenced by the modeling simplifications rather than fully representing a physiological response. Future work should incorporate dynamic brace-anchorage behavior,

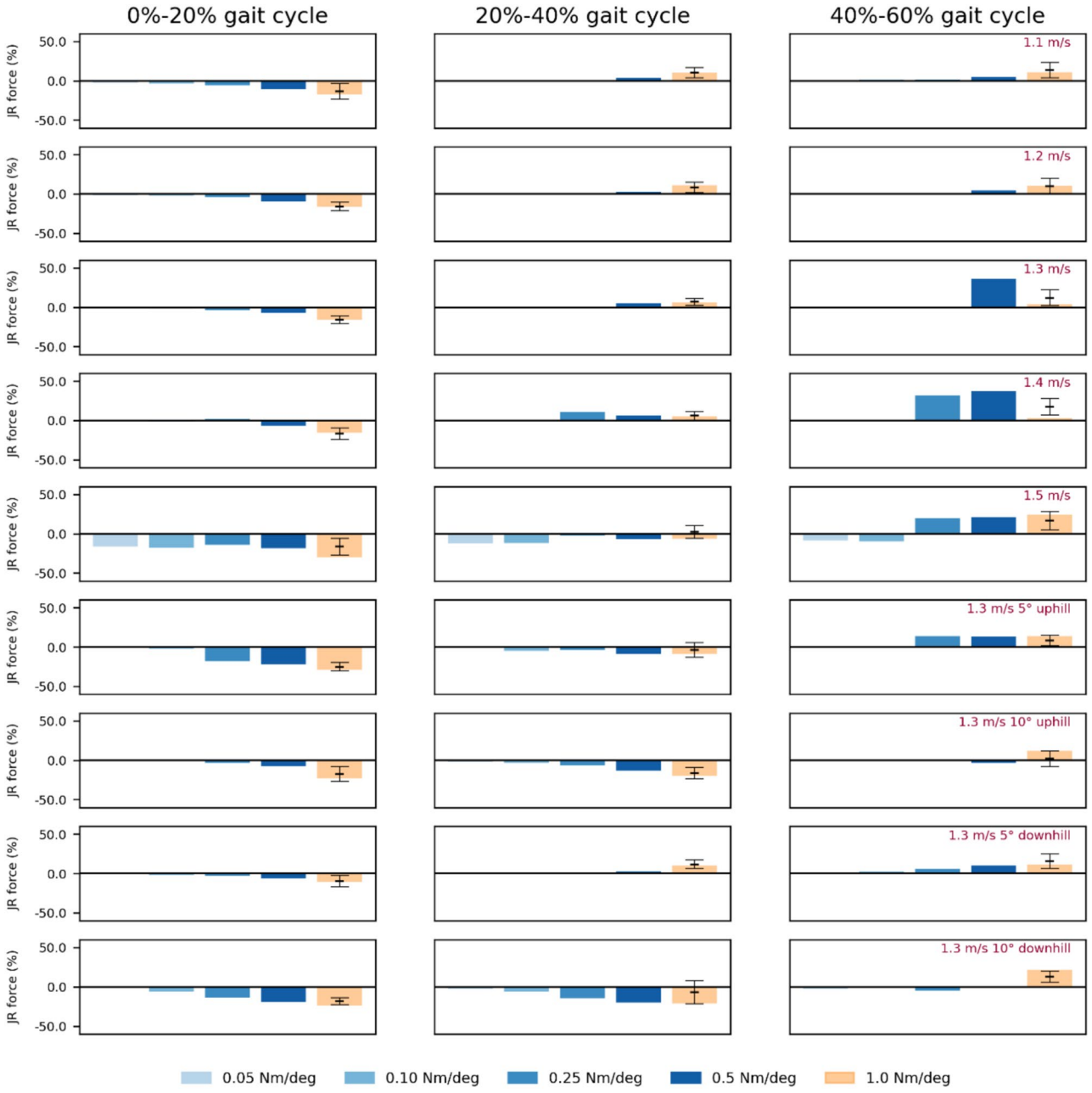

Figure. 8.. Averaged vertical joint reaction (JR) force percentage change relative to baseline of knee joint in stance phase (0–60% gait cycle). Bars show the predictions of the primary model. Horizontal markers and lines denote mean ± standard deviation predicted by additional models under brace stiffness of 1.0 Nm/deg.

including strap elasticity and migration effects, to more accurately estimate the transmitted moment and its neuromuscular consequences. In terms of knee joint modelling, the 2392 OpenSim model assumes a single revolute axis, which provides a simplified representation of knee kinematics. While brace migration could introduce frontal and transverse plane moments under high stiffness conditions, the 1-DoF assumption offers a tractable framework for analysis. Future work may extend this approach to multi-DoF models to capture additional loading components more comprehensively. In this study, direct collocation was selected over other predictive locomotion frameworks (e.g., Scone, MyoSim, LocoMuJoCo) for its proven convergence and flexibility in incorporating brace-stiffness parameters within a physiologically detailed musculoskeletal model. However, future work could explore these alternative frameworks or integrate emerging AI-based algorithms to further enhance efficiency and adaptability.

Conclusions

This study revealed that increasing SLKB stiffness effectively restricted knee range of motion and altered lower-limb kinematics, while simultaneously elevating knee flexor muscle activations to preserve foot clearance. The

unloading effect was phase- and condition-dependent: only high-stiffness SLKBs (1.0 Nm/deg) consistently reduced the first peak of vertical knee joint reaction force during level-ground walking, whereas medium to high stiffness levels produced robust unloading throughout early stance in uphill ambulation, with more variable effects in mid- and late-stance phases and during downhill walking. These findings suggest that targeted use of SLKBs—particularly under incline walking conditions—could enhance joint unloading in patients with knee osteoarthritis. Future work should validate these theoretical results through in vivo trials and explore subject-specific, impedance-controlled brace configurations.

Data availability

All data generated or analyzed during this study are included in this published article.

Received: 21 August 2025; Accepted: 18 December 2025
Published online: 07 January 2026

References

1. Steinmetz, J. D. et al. Global, regional, and national burden of osteoarthritis, 1990–2020 and projections to 2050: A systematic analysis for the Global Burden of Disease Study 2021. *Lancet Rheumatol.* **5**(9), e508–e522. https://doi.org/10.1016/S2665-9913(23)00163-7 (2023).
2. Cudejko, T. et al. The immediate effect of a soft knee brace on dynamic knee instability in persons with knee osteoarthritis. *Rheumatology (Oxford)* **57**(10), 1735–1742. https://doi.org/10.1093/rheumatology/key162 (2018).
3. Ebert, J. R., Hambly, K., Joss, B., Ackland, T. R. & Donnelly, C. J. Does an unloader brace reduce knee loading in normally aligned knees?. *Clin. Orthop. Relat. Res.* **472**(3), 915–922. https://doi.org/10.1007/s11999-013-3297-8 (2014).
4. Liu, M. Q., Anderson, F. C., Schwartz, M. H. & Delp, S. L. Muscle contributions to support and progression over a range of walking speeds. *J. Biomech.* **41**(15), 3243–3252. https://doi.org/10.1016/j.jbiomech.2008.07.031 (2008).
5. Rannou, F., Poiraudeau, S. & Beaudreuil, J. Role of bracing in the management of knee osteoarthritis. *Curr. Opin. Rheumatol.* **22**(2), 218–222. https://doi.org/10.1097/BOR.0b013e32833619c4 (2010).
6. Lee, H., Ha, D., Kang, Y.-S. & Park, H.-S. Biomechanical analysis of the effects of bilateral hinged knee bracing. *Front. Bioeng. Biotechnol.* **4**, 50. https://doi.org/10.3389/fbioe.2016.00050 (2016).
7. D'Lima, D. D., Patil, S., Steklov, N. & Colwell, C. W. The 2011 ABJS Nicolas Andry Award: 'Lab'-in-a-knee: in vivo knee forces, kinematics, and contact analysis. *Clin. Orthop. Relat. Res.* **469**(10), 2953–2970. https://doi.org/10.1007/s11999-011-1916-9 (2011).
8. Bender, A. et al. In vivo load on knee, hip and spine during manual materials handling with two lifting techniques. *J. Biomech.* **163**, 111963. https://doi.org/10.1016/j.jbiomech.2024.111963 (2024).
9. Bishop, E. L. et al. Tricompartment offloader knee brace reduces contact forces in adults with multicompartment knee osteoarthritis. *J. Orthop. Res.* **41**(9), 1925–1933. https://doi.org/10.1002/jor.25556 (2023).
10. McGibbon, C. A., Brandon, S., Bishop, E. L., Cowper-Smith, C. & Biden, E. N. Biomechanical study of a tricompartmental unloader brace for patellofemoral or multicompartment knee osteoarthritis. *Front. Bioeng. Biotechnol.* **8**, 604860. https://doi.org/10.3389/fbioe.2020.604860 (2020).
11. Chen, Z. et al. Effect of component mal-rotation on knee loading in total knee arthroplasty using multi-body dynamics modeling under a simulated walking gait. *J. Orthop. Res.* **33**(9), 1287–1296. https://doi.org/10.1002/jor.22908 (2015).
12. Frigo, C. A. & Donno, L. The effects of external loads and muscle forces on the knee joint ligaments during walking: A musculoskeletal model study. *Appl. Sci.* **11**(5), 2356. https://doi.org/10.3390/app11052356 (2021).
13. Nardini, F. et al. An anatomical-based subject-specific model of in-vivo knee joint 3D kinematics from medical imaging. *Appl. Sci.* **10**(6), 2100. https://doi.org/10.3390/app10062100 (2020).
14. Falisse, A. et al. Rapid predictive simulations with complex musculoskeletal models suggest that diverse healthy and pathological human gaits can emerge from similar control strategies. *J R Soc Interface.* **16**(157), 20190402. https://doi.org/10.1098/rsif.2019.0402 (2019).
15. Porsa, S., Lin, Y.-C. & Pandy, M. G. Direct methods for predicting movement biomechanics based upon optimal control theory with implementation in OpenSim. *Ann. Biomed. Eng.* **44**(8), 2542–2557. https://doi.org/10.1007/s10439-015-1538-6 (2016).
16. Knutzen, K. M., Bates, B. T., Schot, P. & Hamill, J. A biomechanical analysis of two functional knee braces. *Med. Sci. Sports Exerc.* **19**(3), 303–309 (1987).
17. Pierrat, B., Molimard, J., Navarro, L., Avril, S. & Calmels, P. Evaluation of the mechanical efficiency of knee braces based on computational modeling. *Comput. Methods Biomech. Biomed. Engin.* **18**(6), 646–661. https://doi.org/10.1080/10255842.2013.832227 (2015).
18. Wu, X. et al. Finite element analysis of a novel approach for knee and ankle protection during landing. *Appl. Sci.* **11**(4), 1912. https://doi.org/10.3390/app11041912 (2021).
19. Stoltze, J. S. et al. Development and functional testing of an unloading concept for knee osteoarthritis patients: A pilot study. *J. Biomech. Eng.* **144**(1), 011007. https://doi.org/10.1115/1.4051847 (2022).
20. Zhu, A. et al. The effects of brace stiffness on knee joints during pull-up jump shot movements in amateur female basketball players. *Appl. Sci.* **15**(3), 1448. https://doi.org/10.3390/app15031448 (2025).
21. McGibbon, C. A., Brandon, S., Bishop, E. L., Cowper-Smith, C. & Biden, E. N. Biomechanical study of a tricompartmental unloader brace for patellofemoral or multicompartment knee osteoarthritis. *Front. Bioeng. Biotechnol.* **8**, 604860. https://doi.org/10.3389/fbioe.2020.604860 (2021).
22. Hamner, S. R., Seth, A. & Delp, S. L. Muscle contributions to propulsion and support during running. *J. Biomech.* **43**(14), 2709–2716. https://doi.org/10.1016/j.jbiomech.2010.06.025 (2010).
23. Falisse, A., Afschrift, M. & De Groote, F. Modeling toes contributes to realistic stance knee mechanics in three-dimensional predictive simulations of walking. *PLoS ONE* **17**(1), e0256311. https://doi.org/10.1371/journal.pone.0256311 (2022).
24. Serrancoli, G. et al. Subject-exoskeleton contact model calibration leads to accurate interaction force predictions. *IEEE Trans. Neural Syst. Rehabil. Eng.* **27**(8), 1597–1605. https://doi.org/10.1109/tnsre.2019.2924536 (2019).
25. van den Bogert, A. J., Geijtenbeek, T., Even-Zohar, O., Steenbrink, F. & Hardin, E. C. A real-time system for biomechanical analysis of human movement and muscle function. *Med. Biol. Eng. Comput.* **51**(10), 1069–1077. https://doi.org/10.1007/s11517-013-1076-z (2013).
26. Zhou, Y., Wang, X., Tang, X., Ji, X. & Gao, Z. Design and analysis of a passive knee assisted exoskeleton. *Adv. Mech. Eng.* **15**(11), 16878132231202578. https://doi.org/10.1177/16878132231202578 (2023).
27. Chaichaowarat R, Granados DFP, Kinugawa J, Kosuge K, editors. Passive knee exoskeleton using torsion spring for cycling assistance. 2017 IEEE/RSJ International Conference on Intelligent Robots and Systems (IROS); 2017 24–28 Sept. 2017.
28. van der Zee, T. J., Mundinger, E. M. & Kuo, A. D. A biomechanics dataset of healthy human walking at various speeds, step lengths and step widths. *Sci. Data.* **9**(1), 704. https://doi.org/10.1038/s41597-022-01817-1 (2022).

29. Keller, M. et al. From skin to skeleton: Towards biomechanically accurate 3D digital humans. *ACM Transac. Gr.* **42**(6), 253. https://doi.org/10.1145/3618381 (2023).
30. Andersson, J. A. E., Gillis, J., Horn, G., Rawlings, J. B. & Diehl, M. CasADi: A software framework for nonlinear optimization and optimal control. *Math. Program. Comput.* **11**(1), 1–36. https://doi.org/10.1007/s12532-018-0139-4 (2019).
31. Falisse, A., Serrancolí, G., Dembia, C. L., Gillis, J. & De Groote, F. Algorithmic differentiation improves the computational efficiency of OpenSim-based trajectory optimization of human movement. *PLoS ONE* **14**(10), e0217730. https://doi.org/10.1371/journal.pone.0217730 (2019).
32. Wächter, A. & Biegler, L. T. On the implementation of an interior-point filter line-search algorithm for large-scale nonlinear programming. *Math. Program.* **106**(1), 25–57. https://doi.org/10.1007/s10107-004-0559-y (2006).
33. Seth, A. et al. OpenSim: Simulating musculoskeletal dynamics and neuromuscular control to study human and animal movement. *PLoS Comput. Biol.* **14**(7), e1006223. https://doi.org/10.1371/journal.pcbi.1006223 (2018).
34. Fregly, B. J. et al. Grand challenge competition to predict in vivo knee loads. *J. Orthop. Res.* **30**(4), 503–513. https://doi.org/10.1002/jor.22023 (2012).
35. Greene, P. J. & Granat, M. H. The effects of knee and ankle flexion on ground clearance in paraplegic gait. *Clin. Biomech. (Bristol).* **15**(7), 536–540 (2000).
36. Stoltze, J. S., Oliveira, A. S. C., Rasmussen, J. & Andersen, M. S. Evaluation of an unloading concept for knee osteoarthritis: A pilot study in a small patient group. *J. Biomech. Eng.* https://doi.org/10.1115/1.4064031 (2024).
37. Geyer, H. & Herr, H. A muscle-reflex model that encodes principles of legged mechanics produces human walking dynamics and muscle activities. *IEEE Transac. Neural Syst. Rehabil. Eng. Publ. IEEE Eng. Med. Biol. Soc.* **18**(3), 263–273. https://doi.org/10.1109/TNSRE.2010.2047592 (2010).
38. Kuster, M., Sakurai, S. & Wood, G. A. Kinematic and kinetic comparison of downhill and level walking. *Clin. Biomech. (Bristol).* **10**(2), 79–84 (1995) (**PubMed PMID: 11415535**).
39. Kwee-Meier, S. T., Mertens, A. & Jeschke, S. Age-induced changes in the lower limb muscle activities during uphill walking at steep grades. *Gait Posture* **62**, 490–496. https://doi.org/10.1016/j.gaitpost.2018.04.003 (2018).

Author contributions

Kuan Wang: Conceptualization, Methodology, Software, Writing- Original draft preparation. Xinpeng Chen: Software. Linlin Zhang: Data curation. Leichao Liang: Visualization. Xiaoyue Hu: Software. Huihao Wang: Writing- Reviewing and Editing, Supervision.

Funding

This work was supported by Shanghai Municipal Health Commission Excellent Young Medical Talents Training Program (No. 2022YQ038), and partially supported by SUMHS Faculty Talent "Hundred-Person Pool" Project (A1-0200-25-311007-11), SUMHS Faculty Teaching and Research Project (A1-0200-25-309009-3), Young Teachers Training and Support Program for Shanghai Higher Education Institutions (A1-0200-25-311001-17, A1-0200–25-311001-18), National Natural Science Foundation of China (31900942, 82575085), Natural Science Foundation of Shanghai (No. 20ZR1452600).

Declarations

Competing interests

The authors declare no competing interests.

Additional information

Supplementary Information The online version contains supplementary material available at https://doi.org/10.1038/s41598-025-33424-6.

Correspondence and requests for materials should be addressed to K.W. or H.W.

Reprints and permissions information is available at www.nature.com/reprints.

Publisher's note Springer Nature remains neutral with regard to jurisdictional claims in published maps and institutional affiliations.